CHAPTER-8

(Synthesis and Characterisation of Porous ZrO_2-Spinel)

8.1 Synthesis of Porous $MgO-Al_2O_3-ZrO_2$

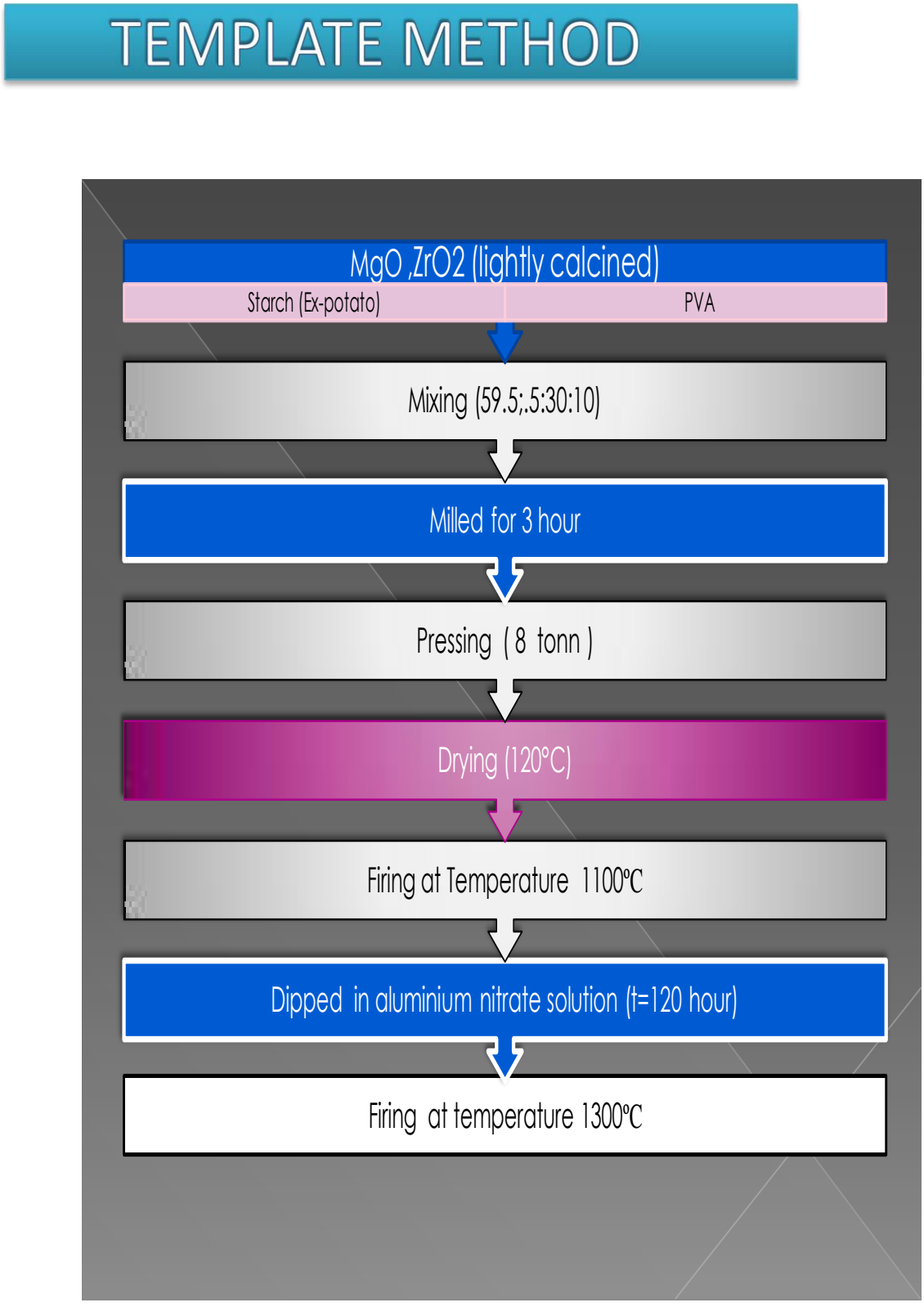

8.1 Block diagram of Zircon Porous Spinel

8.2 Characteristics of Porous $MgO-Al_2O_3-ZrO_2$

From Figure 8.1 Dilatometrics expansion it is clear that coefficient of thermal expansion grow to be stable subsequent to a temperature superior than 600°C. From figure 8.2 Thermal conductivity of a sample are considered by scorching line method .Thermal conductivity of ZPSP were 4.7 w/mk [Tian *et al,*2009]

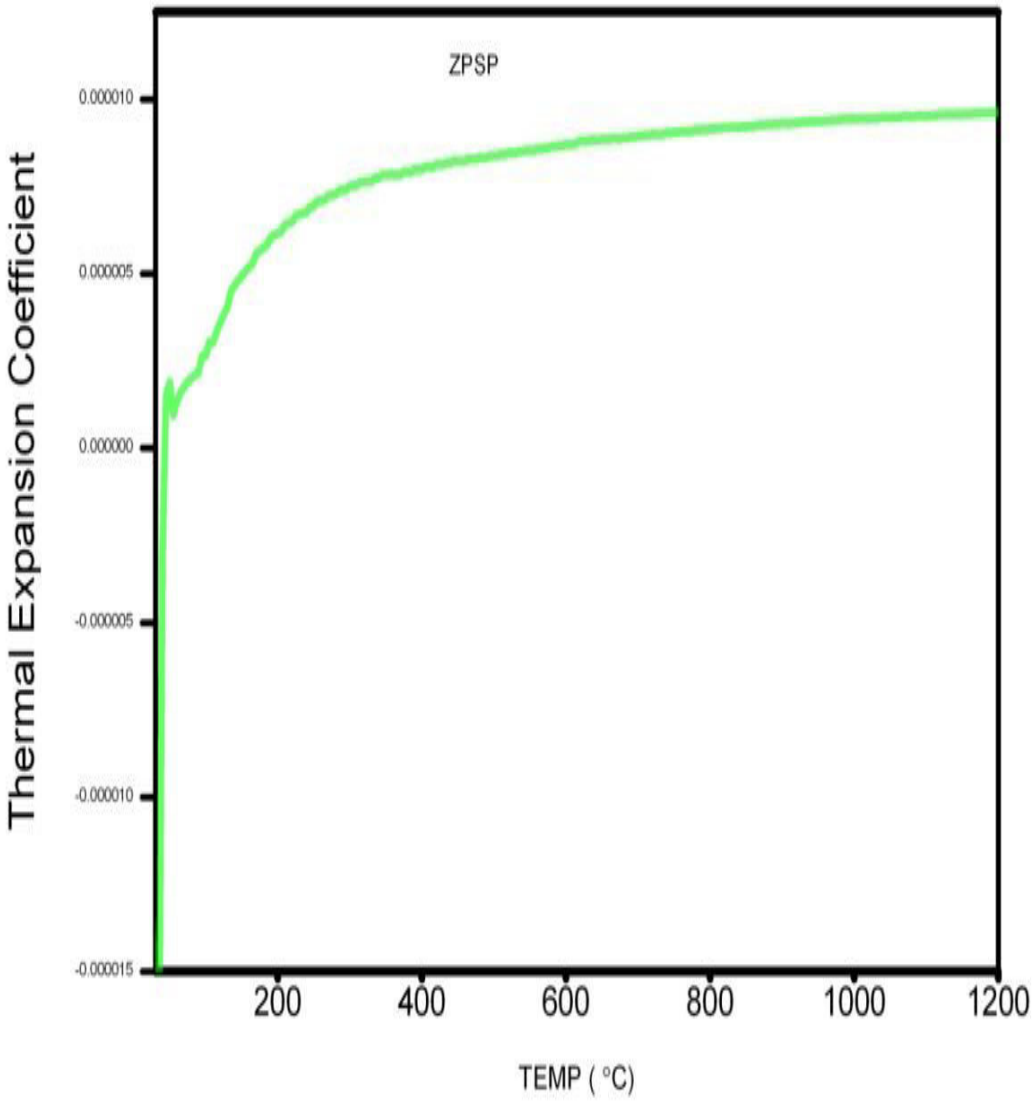

Figure 8.1 Coefficient of thermal expansion for zircon porous spinel

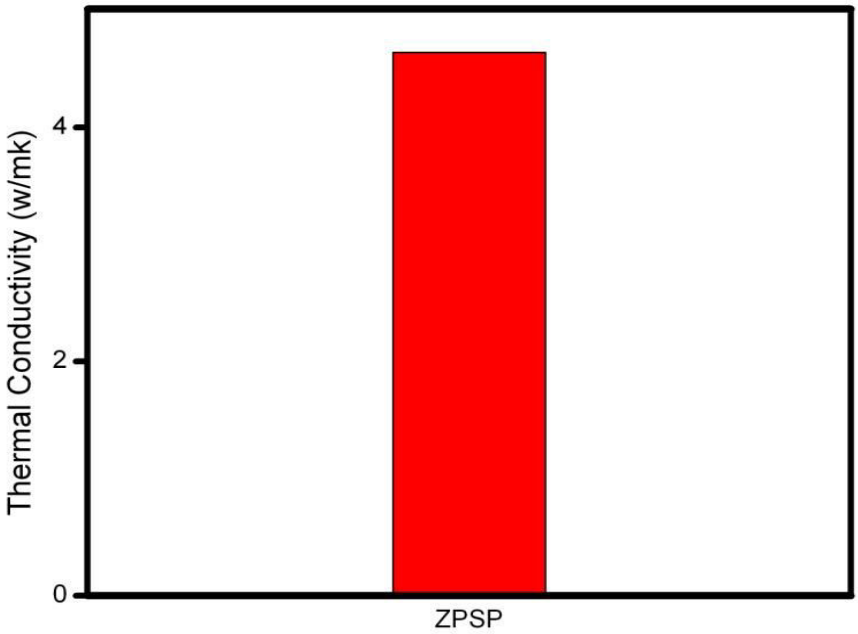

Figure 8.2 Thermal Conductivity for zircon porous spinel

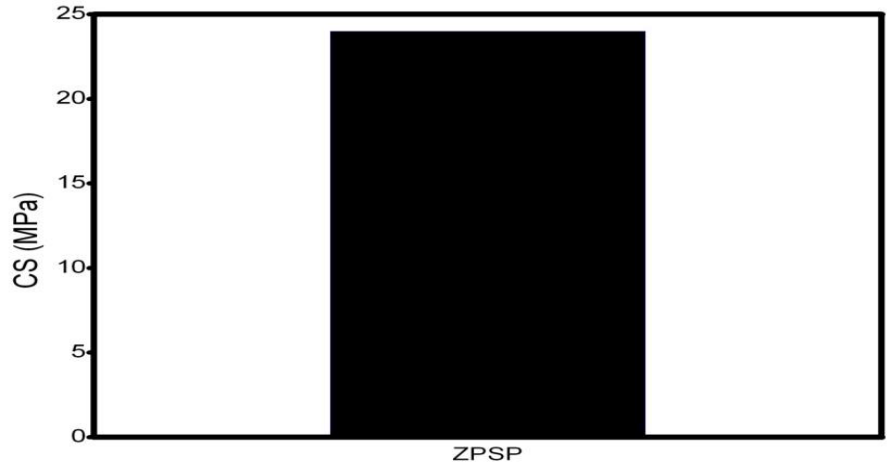

Figure 8.3 Compressive strength for ZPSP

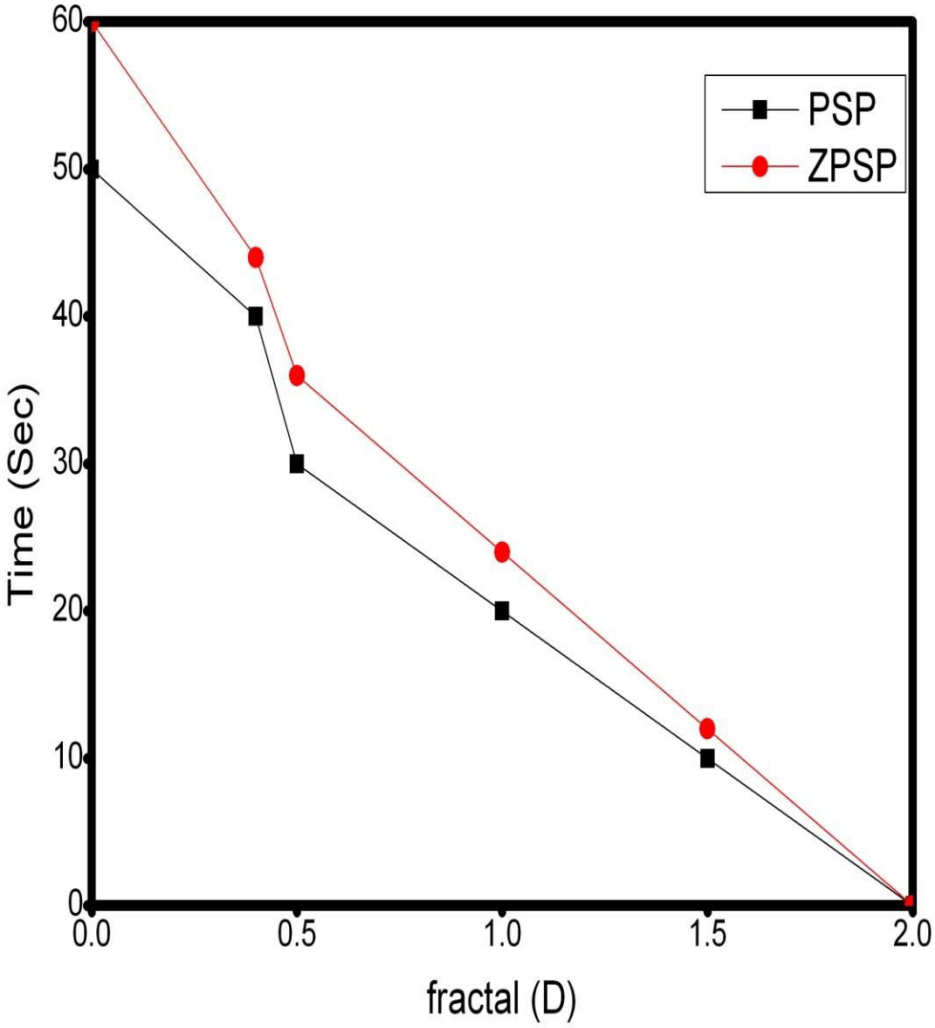

Figure 8.4 comparatively study of fractal structure of PSP and ZPSP

From the Figure 8.3 Compressive strength of ZPSP were measured 24 MPa. From the Figure 8.4 it is clear that When a transient time response signal are passes through the ZPSP, fractal topology D=2 are quick change to D=0 As comparison to PSP due to addition of zirconia in a absorbent spinel. [Slovak, (2002)]

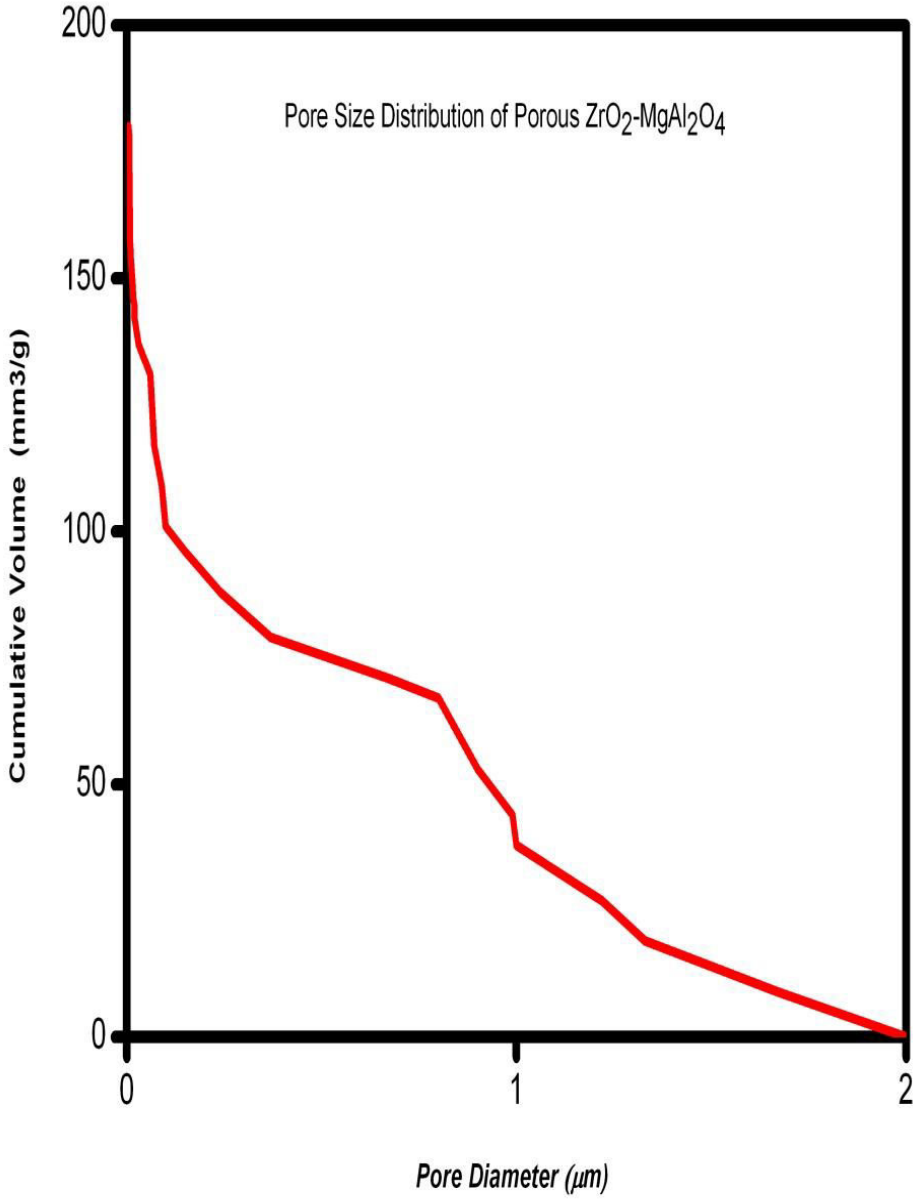

Figure 8.5 Pore size distribution of ZPSP

From the given Figure 8.5 it is clear that Some pore size are grater than 1 micro meter where as some pore are less than 1 micrometer the pore shape show non uniform distribution. we also find some pore of nano range in wide amount. Pore shape are in 0-2 micrometer range.

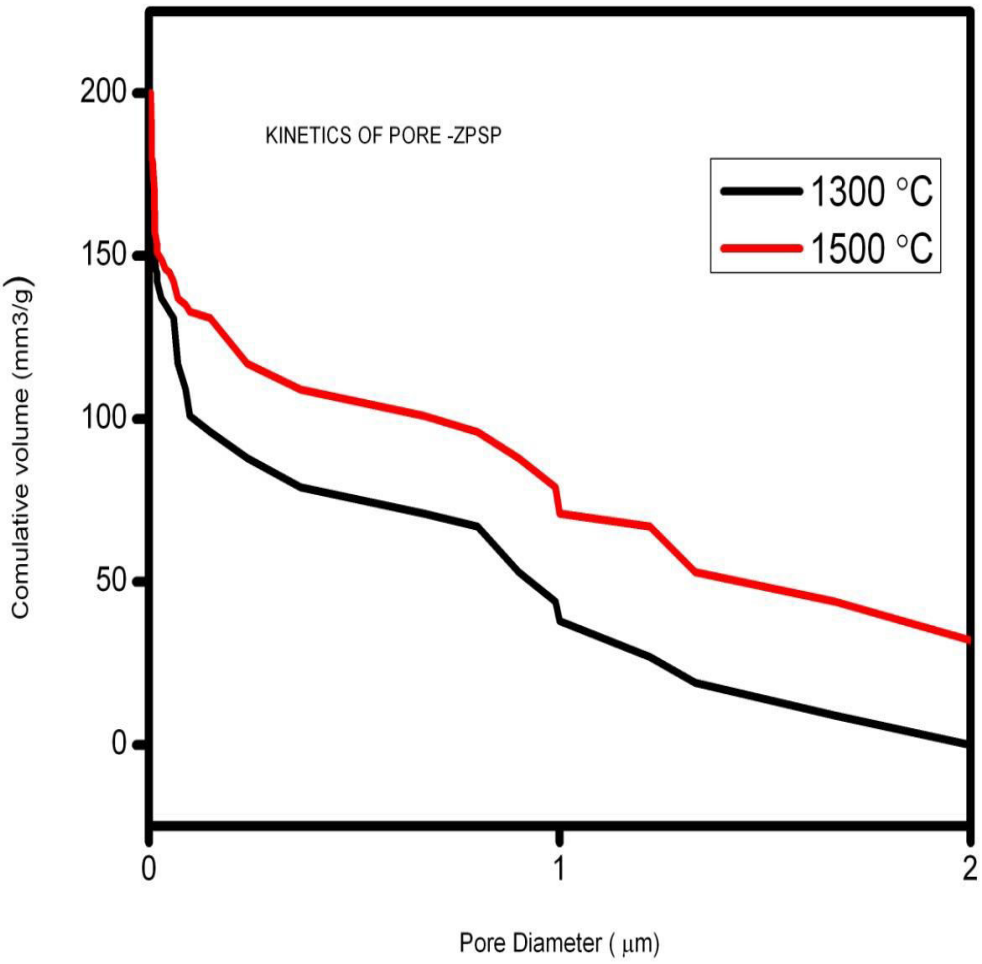

Figure 8.6 Kinetics Pore size distribution of ZPSP

From the Figure 8.6 as the temp is Increases the number of accumulation Pore are slightly increases,means several pore satuated at one place only. Gathering of orifice size greater than 2 micro meter are furthermore increases owing to rise in temperature.

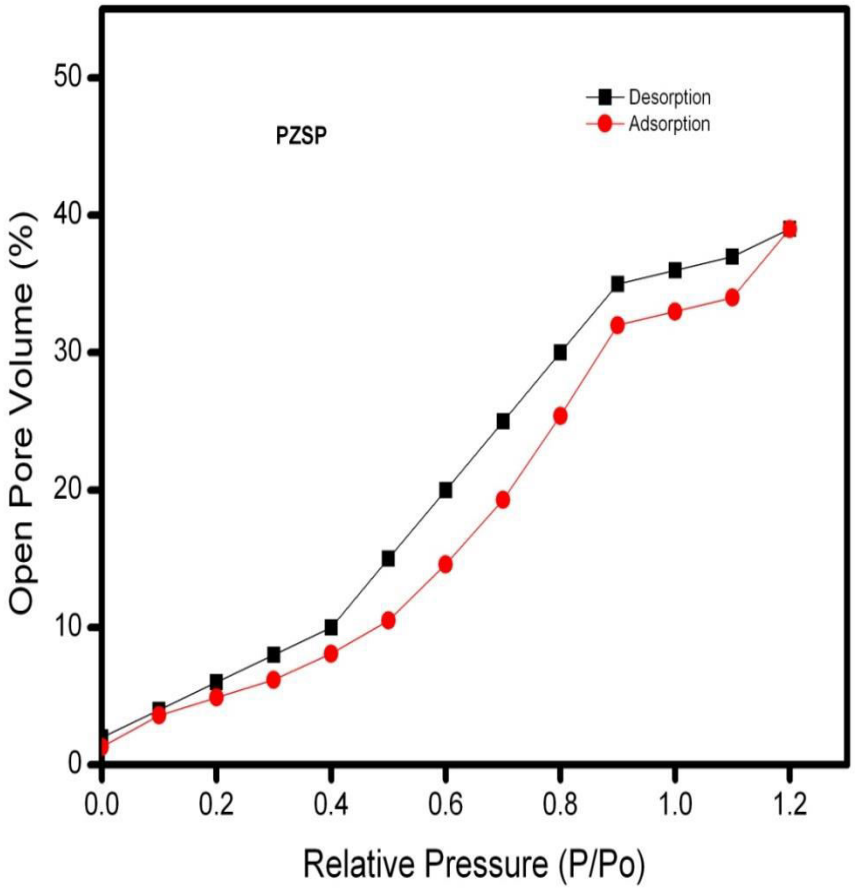

Figure 8.7 Adsorption and desorption isotherm and corresponding pore size distribution of sample –ZPSP

From the given Figure 8.7 it is clear that porosity of ZPSP is 39% .The porosity are decreases when we added small amount of zirconia to absorbent spinel.

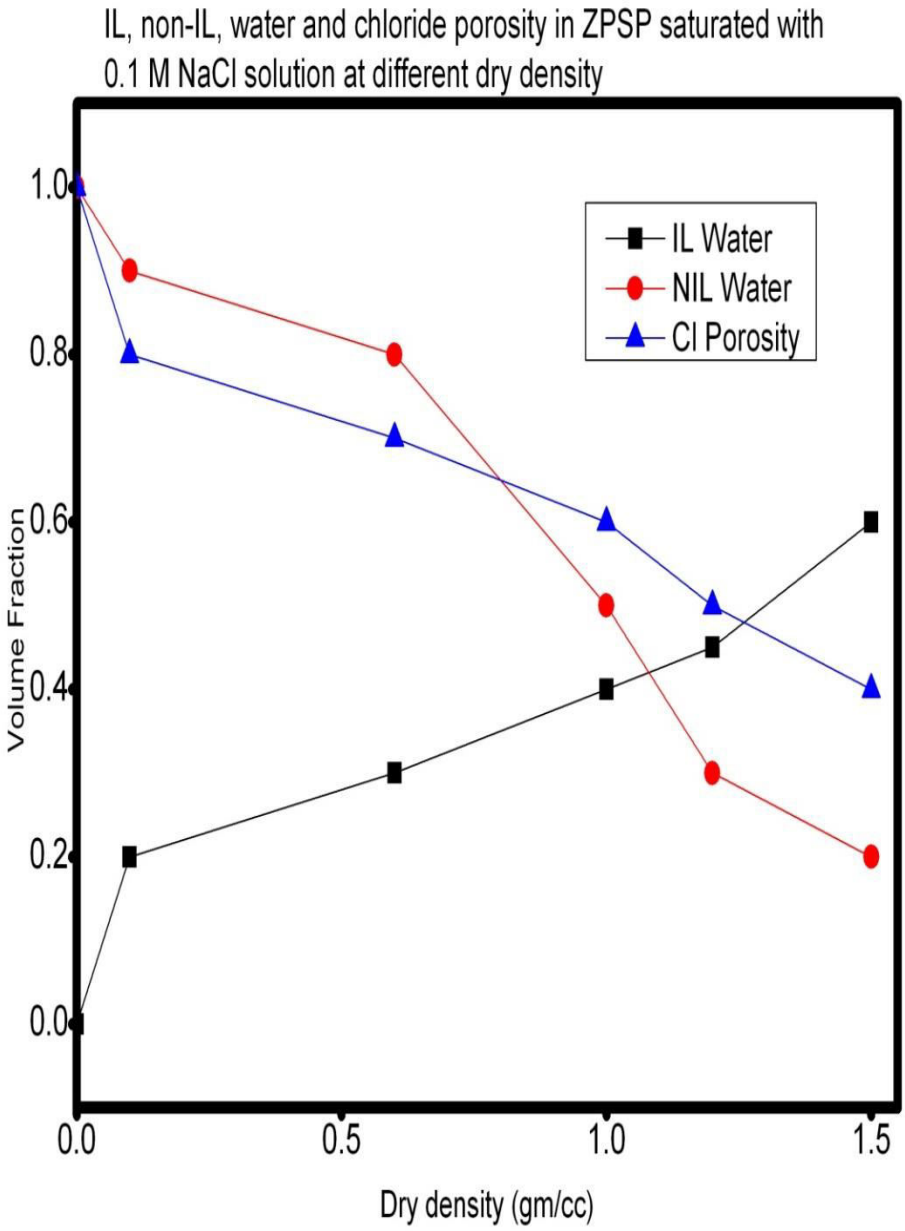

Figure 8.8 volume fraction by addition of Cl in ZPSP

From the figure 8.8 Minute are filled with IL ,NIL and CL porosity in ZPSP drenched with .1 M Na Cl with unusual density volume fraction are decline in case of Cl porosity where IL water percentage are decreases.

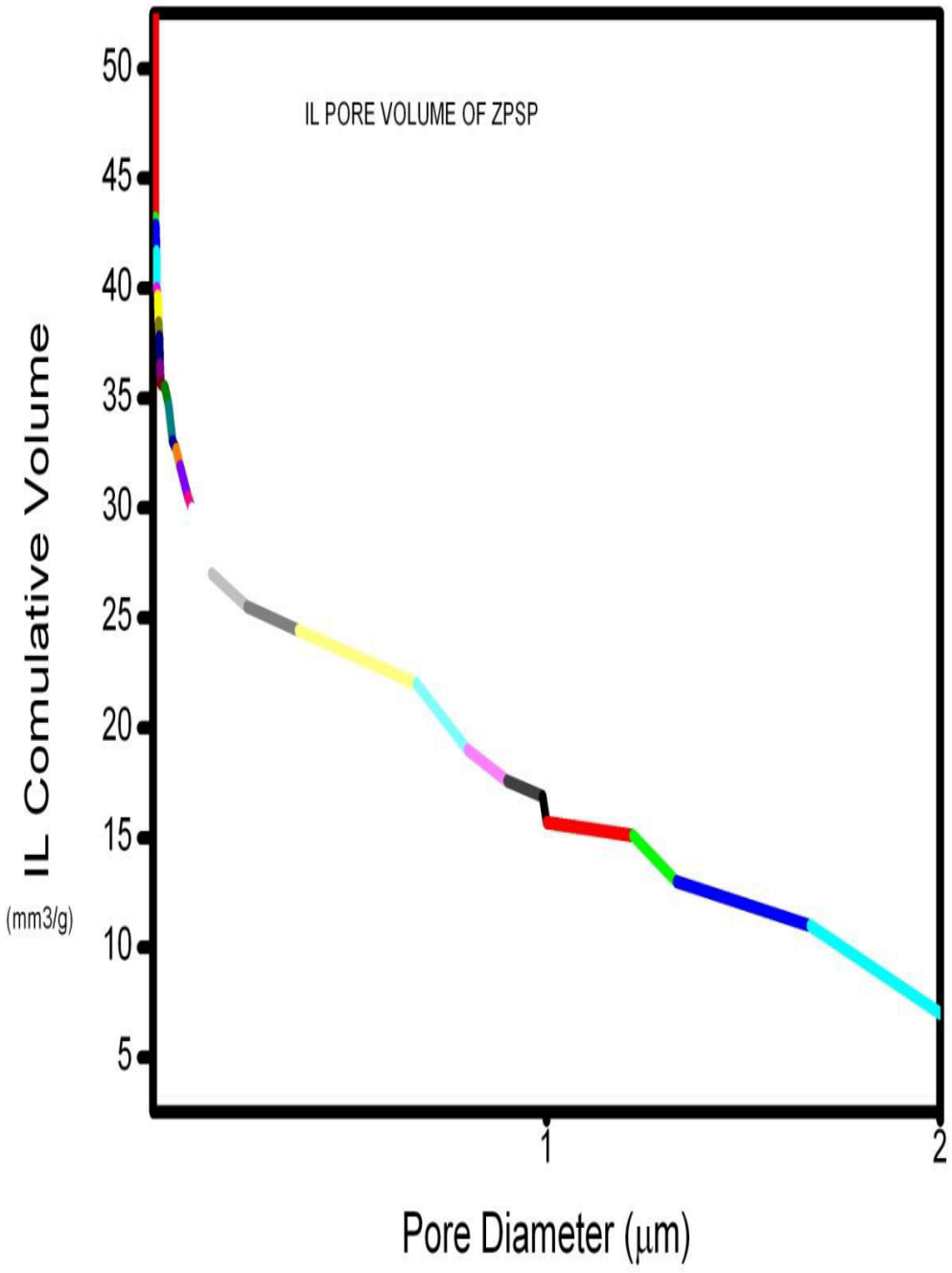

Figure 8.9 IL Pore volume of ZPSP

From the above it is clear thar the IL Comulative pore is greater in case of nano meter pore diameter range. Pore size distribution are Non uniform accoumulation [Cacrew, (1959)].

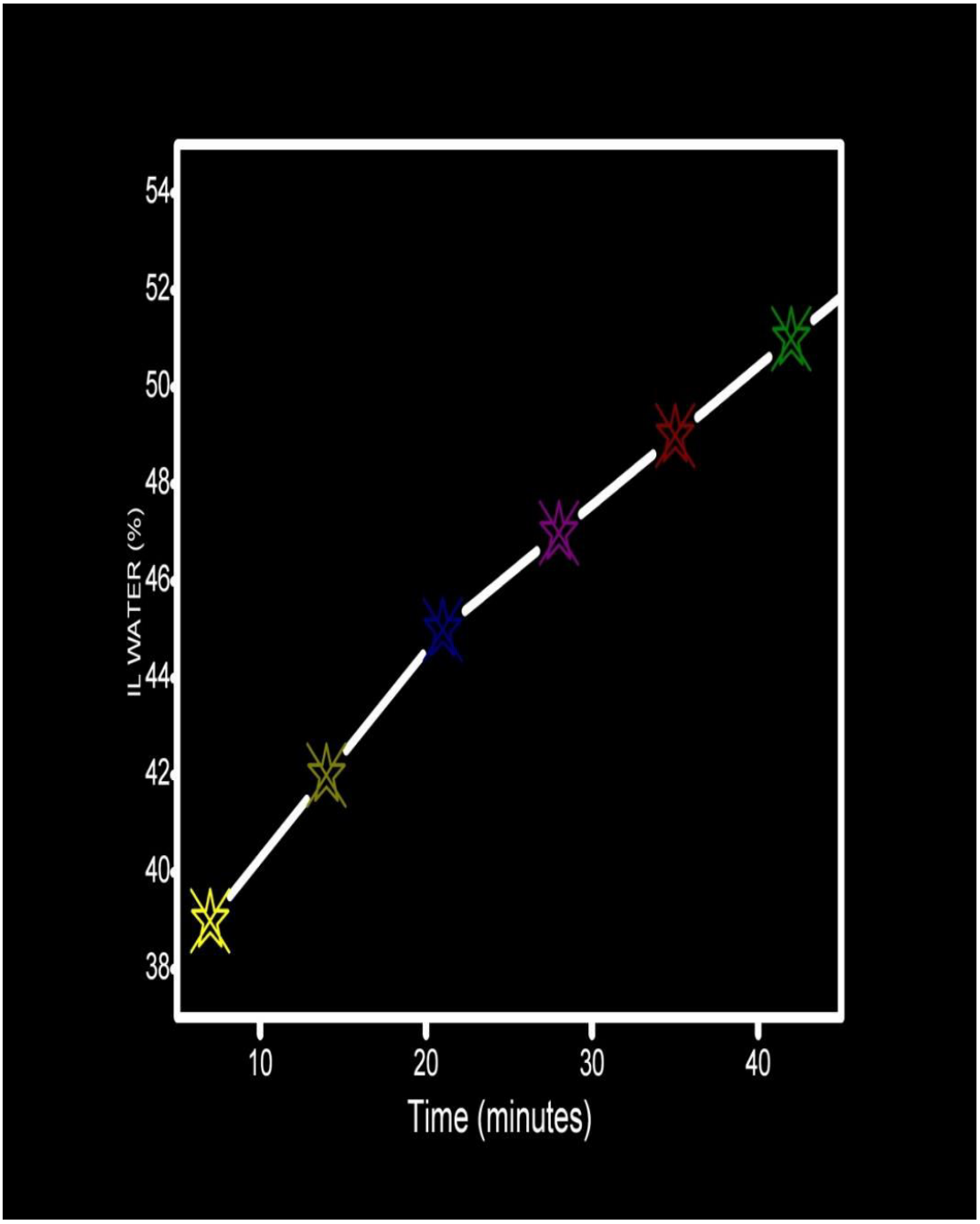

Figure 8.10 Relation ship between IL Water and Time in minutes

Figure 8.10 shows relation ship between IL water and time in minutes it is maximum for 5 solution treatment.The IL water is 38% for PMSO solution treatments are given .IL water is 51% for PMS5 [Grzelczak ,(2013)].

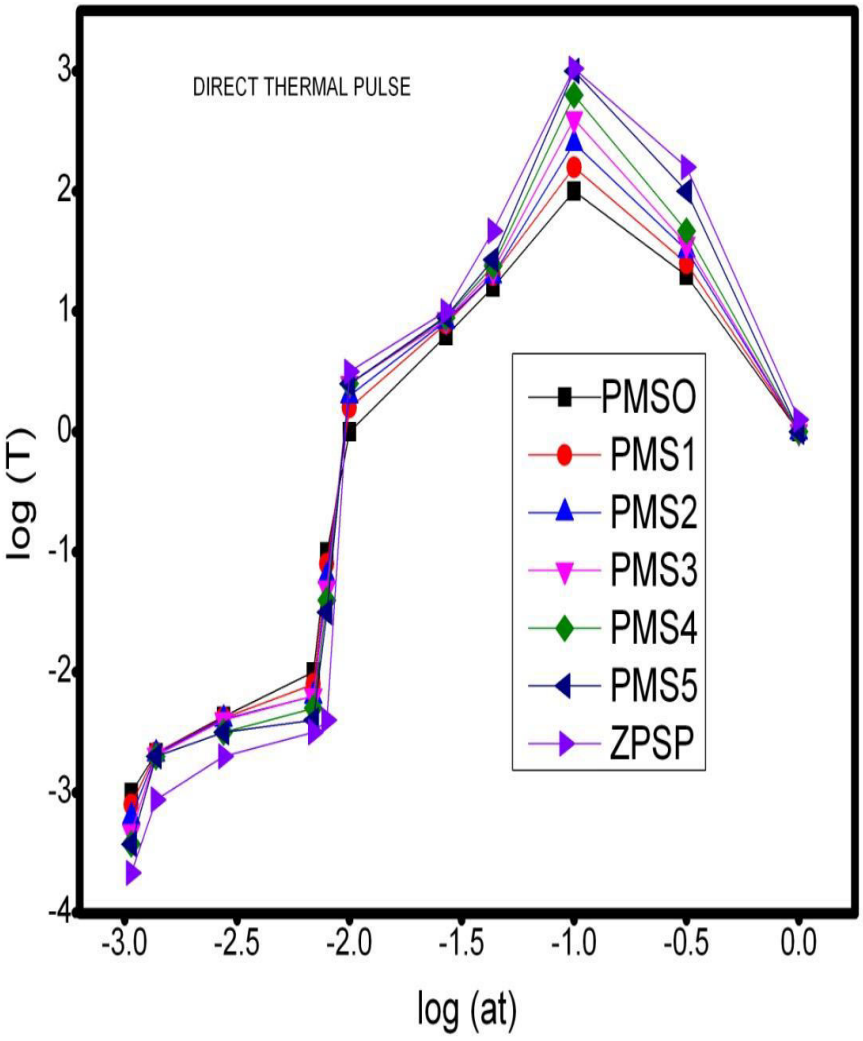

Figure 8.11.Direc thermal pulse response curve on ZPSP and porous MgO with different solution treatments

From the above figure A Direc thermal pulse provides a maximum response in case of ZPSP having high thermal response in term of thermal diffisuvity,thermal conductivity and specific

heat capacity .Direc thermal pulse are use to determined the maximum diffusivity and fractal measurement of material [Cacrew, (1959)] .

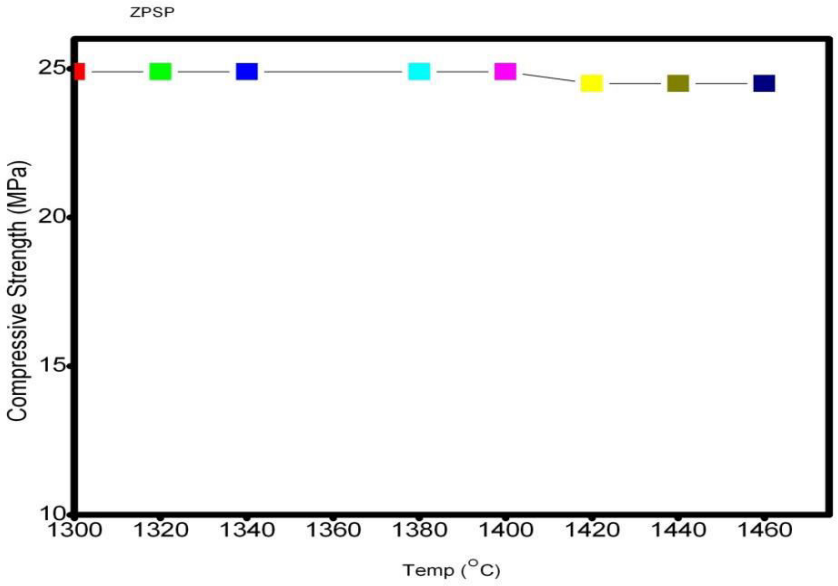

Figure 8.12 Measurement of compressive strength for thermal shock

From the Figure 8.12 and 8.13 When sucessively measured a compressive strength at regular Temperature ,we getting a sharp decrease in strength at interval 1400 to 1420 there is thermal shock due to this strength of material are decrease [Cacrew, (1959)].

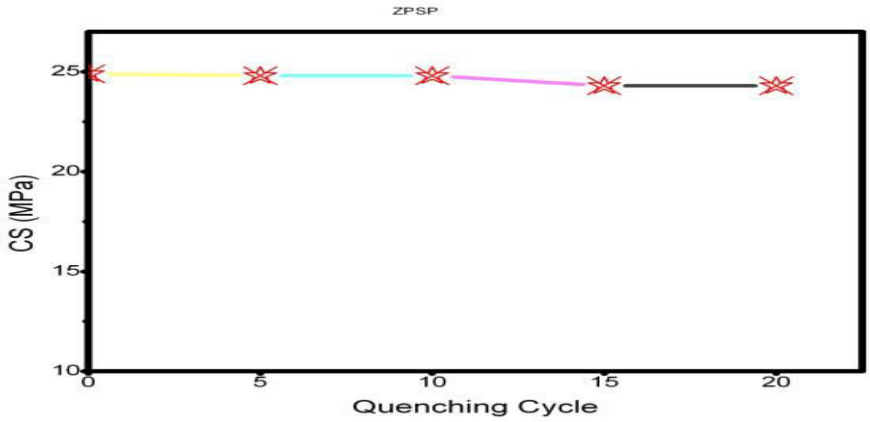

Figure 8.13 Coverage of compressive strength for thermal shock in singular extinguish rotation

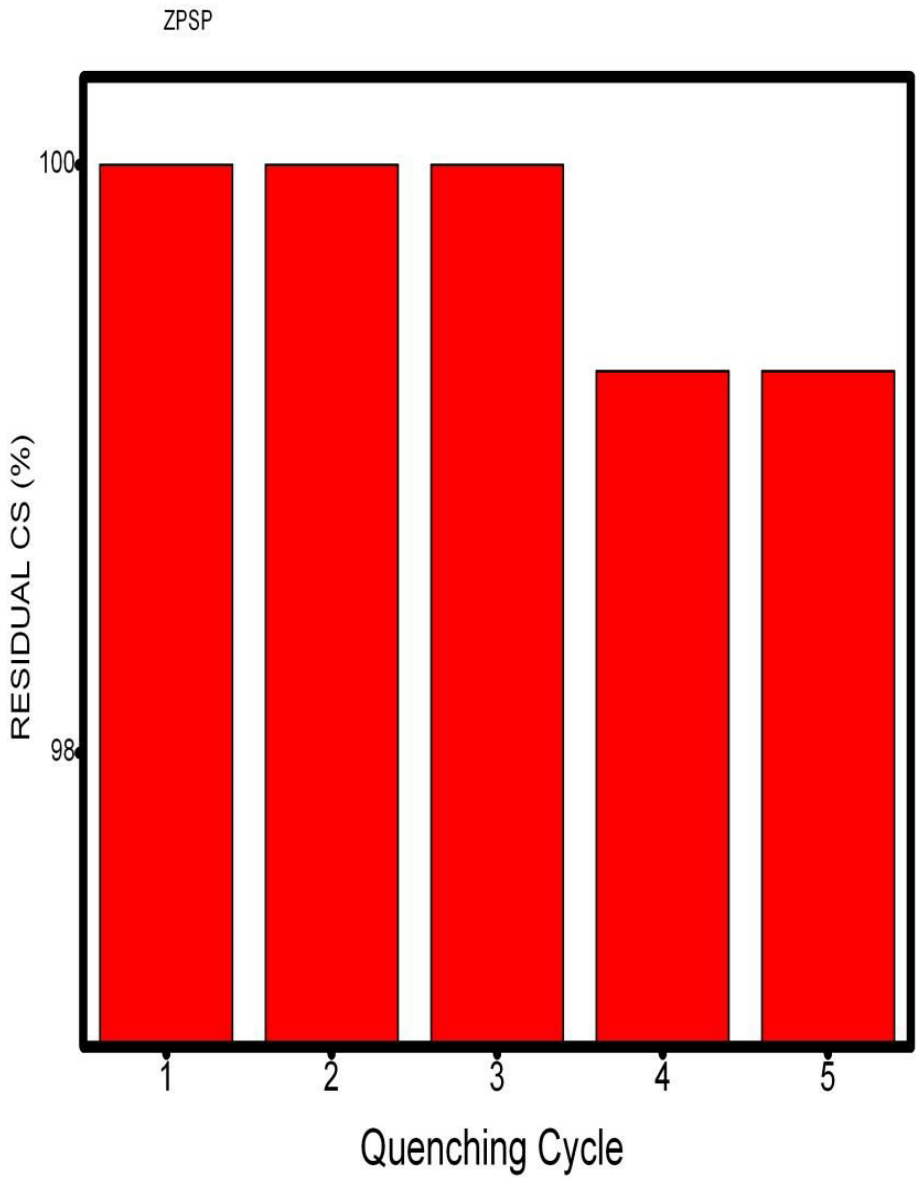

Figure 8.14 Residual compressive strength for different quenching cycle

Figure 8.14 Shows Residual compressive strength is maximum for first cycle and minimum for fifth cycle .The quenching cycle graph of zirconia porous spinel are given.